JOURNAL OF NATURAL PRODUCTS

Article

pubs.acs.org/jnp

Structural Characterization and Antimicrobial Evaluation of Atractyloside, Atractyligenin, and 15-Didehydroatractyligenin Methyl Ester

Federico Brucoli,* Maria T. Borrello, Paul Stapleton, Gary N. Parkinson, and Simon Gibbons

UCL School of Pharmacy, London, WC1N 1AX, U.K.

Supporting Information

ABSTRACT: We report the first complete structure elucidation of the *ent*-kaurane diterpenoid glycoside atractyloside (**1**) by means of NMR and X-ray diffractometry techniques. Extensive one- and two-dimensional NMR experiments were employed to assign the proton and carbon signals of **1**, and crystallography experiments established the configurations of all stereogenic centers. Furthermore, we present a novel semisynthetic route for the preparation of the highly cytotoxic aglycone derivative of **1**, 15-didehydroatractyligenin methyl ester (**3**). All compounds were tested for their antibiotic activity against *Enterococcus faecalis*, *Escherichia coli*, and several strains of *Staphylococcus aureus*, including fluoroquinolone-resistant (SA1199B) and two epidemic MRSA (EMRSA-15 and -16) strains. Compound **3** exhibited moderate activity against all of the *Staph. aureus* strains with an MIC value of 128 mg/L.

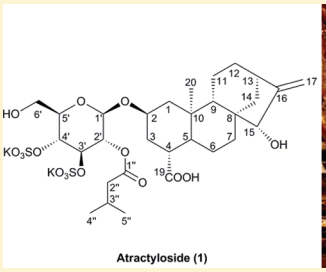

Atractylis gummifera L. (Asteraceae) is a thistle that grows throughout the Mediterranean region and is widely known for its acute toxicity.[1,2] Accidental ingestion of *A. gummifera* rhizomes still remains a cause of human poisoning, particularly during the spring or winter, when the content of the active plant principles, atractyloside (**1**) and its C-4 dicarboxylic acid derivative, carboxyatractyloside, are higher.[3,4] Atractyloside (**1**) was first isolated by Lefranc in 1868 from the roots of *A. gummifera*,[5] and several other atractyloside analogues, which all contain its aglycone derivative atractyligenin (**2**), were recently discovered in *Callilepsis laureola*,[6] *Widelia glauca*,[7] and species of various coffee plants (*Coffea arabica* and *Coffea robusta*).[8,9] The glucoside atractyloside consists of the tetracyclic *ent*-kaurane diterpene genin **2** attached through a *β*-linkage to the anomeric carbon of the D-(+)-glucose residue. Only one hydroxy group is free in the carbohydrate moiety (C-6′), while the others are either linked to a residue of isovaleric acid (C-2′) or transformed into two sulfate moieties (C-3′ and C-4′) (Figure 1).[10−12]

The mechanism of action of atractyloside and carboxyatractyloside has been elucidated and involves the inhibition of oxidative phosphorylation in the mitochondria of hepatocytes and proximal tubular epithelial cells.[13] These glucosides block the transport of adenosine diphosphate (ADP) into mitochondria by inhibiting the adenine nucleotide translocator (ANT) and impairing ATP production in the cell.[14,15] Atractyligenin (**2**) exerts similar, albeit weaker, biological activity compared to **1** and is about 150-fold less toxic,[13] suggesting that the glucose moiety and disulfuric and isovaleric acid residues increase the inhibitory effect on ATP production. Atractyloside (**1**) and atractyligenin (**2**) exhibit modest antiproliferative activity

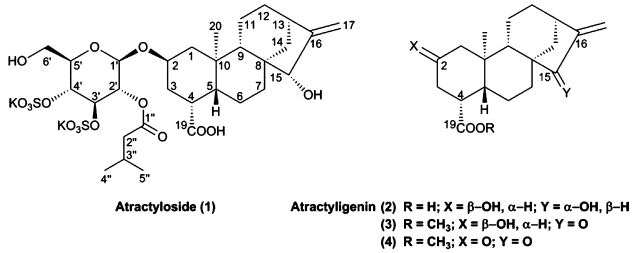

Figure 1. Structures of atractyloside (**1**), atractyligenin (**2**), and 15-didehydro- (**3**) and 2,15-di(didehydro)-atractyligenin methyl ester (**4**) derivatives.

against murine melanoma and metastatic (B-16)[16] and human chronic myelogenous leukemia (K-562)[17] cell lines, respectively. NMR structure elucidation of atractyloside (**1**) has been only partially achieved to date, and previous ^{1}H NMR spectroscopic data of **1** in DMSO-d_6 at 100 MHz reported only signals of H-1′, H-2′, H-3′, and H-4′ of the glucosyl moiety, *ent*-kaurane H_2-1, H-2, H_2-3, and H-4, *exo*-methylene H_2-17 (2H), and methyl CH_3-20 (3H).[7,13] Furthermore, NMR spectroscopy studies on the interactions of atractyloside with the mitochondrial ANT carrier reported incomplete carbon and no proton resonance assignments for **1**.[18] On the other hand, early resonance assignments made for carboxyatractyloside might provide a general reference for structure elucidation of the carbon skeleton of **1**.[19]

Received: January 27, 2012
Published: May 17, 2012

More recently, some naturally occurring and semisynthetic tetracyclic *ent*-kaurane diterpenoids, structurally related to **1** and **2**, have attracted attention due to their interesting anticancer, antibacterial, and anti-inflammatory activity.[20−22] In particular, a semisynthetic derivative of atractyloside (**1**), 15-didehydroatractyligenin methyl ester (**3**), exhibited significantly higher cytotoxicity against selected cancer cell lines compared to **1** and **2** (Figure 1).[22] This compound (**3**) contains in its molecular framework an *exo*-methylene group (C-16−C-17) conjugated with a carbonyl residue (C-15) and may exert its biological activity by acting as a Michael-type acceptor compound, with the α,β-unsaturated carbonyl system serving as the alkylating center.[23]

In this paper, we present the first complete structural characterization of **1** by NMR spectroscopy and X-ray crystallography. Results from ^{1}H and ^{13}C NMR spectra and COSY, NOESY, HSQC, and HMBC experiments were analyzed and employed to assign all carbon and proton signals of **1**. Crystallography experiments allowed evaluation of the atomic spatial arrangement of three independent molecules of **1** in the non-centrosymmetric space group $C\ 2\ 2\ 2_1$ and the determination of their absolute structures and configurations.

We also report some synthetic modification of the atractyloside structure including a novel semisynthetic route for the preparation of the highly cytotoxic derivative **3** starting from **1**. Selective oxidation of the 15-hydroxy group of **1** afforded compound **3** in good yield and purity, with an intact C-2 hydroxy group. The presence of a free hydroxy group in the molecule is a prerequisite for coupling with different residues, including various carbohydrate moieties, to improve its biological activity. The hydroxy group could also be amenable to enzymatic transformation within the cell or could be available to hydrogen-bond with H-acceptors of protein/DNA base pairs.

Finally, compounds **1**−**3** were evaluated for their antimicrobial activities against a number of Gram-positive cocci, including *Enterococcus faecalis* and different strains of methicillin- (MRSA) and antibiotic-resistant *Staphylococcus aureus*, and Gram-negative bacilli such as *Escherichia coli*.

RESULTS AND DISCUSSION

Synthetic modification of the atractyloside structure started with the hydrolysis of its glycosidic bond under basic conditions to give atractyligenin (**2**) (Scheme 1). The genin was characterized by NMR spectroscopy, and the assignments of its proton and carbon signals served as a reference in the NMR structure elucidation of **1** (Table 1).

Next, attention was focused on the synthesis of the 15-didehydroatractyligenin derivative **3**. Previous attempts to prepare **3** from atractyligenin methyl ester were partially efficient. Direct oxidation of the latter with MnO_2 led to a mixture of 15-didehydro- (**3**) and 2,15-di(didehydro)-atractyligenin methyl ester (**4**) derivatives (Figure 1).[21] A novel synthetic route for the preparation of **3** was developed, and selective oxidation of the C-15 hydroxy group was achieved utilizing the carbohydrate moiety of **1** as a protective group for the C-2 hydroxy group (Scheme 1). Methylation of **1** at C-19 using (trimethylsilyl)diazomethane ($TMSCH_2N_2$) gave atractyloside methyl ester **5**. The ^{1}H NMR spectrum of **5** showed the presence of both methyl ester and carbohydrate proton signals, indicating that it still comprised both the sugar and *ent*-kaurane moieties. At this stage, the original strategy would involve oxidation of the C-15 hydroxy group with the Dess-Martin

Scheme 1[a]

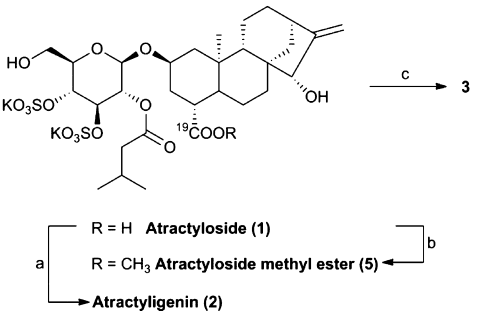

[a]Reagents and conditions: (a) 20% KOH in H_2O, 100 °C, 6 h; (b) $TMSCH_2N_2$, THF/MeOH (4:1 v/v), −78 °C to rt, 3 h; (c) DMP, CH_2Cl_2, 0 °C to rt, 3 h.

periodinane (DMP) and enzymatic or acidic cleavage of the glycosidic bond to give **3**. However, the use of an excess of DMP not only oxidized the C-15 hydroxy group but also cleaved the glycosidic bond, gratifyingly affording the 15-didehydro derivative **3** in two synthetic steps. The ^{1}H and ^{13}C NMR spectra of **3** showed the methyl ester signal at δ_H 3.67, the two broad methylene singlets at δ_H 5.95 and 5.26, which were shifted downfield compared to **1** and **2**, and the C-15 carbonyl at δ_C 210.2, confirming the completion of the reaction.

The unexpected oxidative cleavage of the glycosidic bond might take place as a side-reaction during the quenching of the oxidation reaction with concentrated aqueous NaOH solution. A possible mechanism is shown in Scheme 2. After oxidation of the C-15 alcohol group of **5**, the 15-oxokaurenoic and glucose residues were still joined by a glycosidic bond in **6**. Attack of the heterocyclic oxygen of **6** to iodinane (DMP) led to the formation of complex **7** with loss of an acetate ligand. This unstable intermediate (**7**) might be susceptible to cleavage of the pyranose ring by hydroxide ion and hydrolysis of residues R_2 and R_3 at C-2′, C-3′, and C-4′ to give **8**. Deprotonation at the C-1′ proton by an acetate ion would subsequently afford the pyranose derivative **9**, iodinane, and acetic acid. Finally, intramolecular esterification yielded δ-gluconolactone **10** and the 15-oxo derivative **3**. The proposed mechanism was corroborated by the presence of traces of δ-gluconolactone in the ^{1}H NMR spectrum of the $CHCl_3$ extracts of the neutralized aqueous solution after workup. No anomeric proton signals were detected in this spectrum.

The main challenge in determining the structure of atractyloside (**1**) by NMR spectroscopy was posed by the overlapping signals of nine protons pertaining to its *ent*-kaurane residue. The ^{1}H NMR spectrum of **1** in DMSO-d_6 at 500 MHz showed crowded regions at δ_H 1.56−1.49 (spin system A) and δ_H 1.38−1.28 (spin system B), integrating for four and five protons, respectively. Two-dimensional heteronuclear NMR experiments showed correlations between the A and B system protons and six carbon signals, including five methylene groups and one methine carbon. ^{1}H−^{13}C HSQC−DEPT135 experiments revealed that the methylene carbon signals at δ_C 17.5, 32.1, and 34.7 correlated with two protons each in systems A and B. These carbon signals were assigned to C-11, C-12, and C-7, respectively. The methylene carbon signal at δ_C 24.9 correlated with one multiplet at δ_H 1.78−1.73 (1H) and to one A spin system proton and was assigned to C-6. The methylene signal at δ_C 35.7 correlated with the overlapped doublet at δ_H 1.70 and with one B system proton and was assigned to C-14.

dx.doi.org/10.1021/np300080w | J. Nat. Prod. 2012, 75, 1070−1075

Table 1. ^{1}H and ^{13}C NMR Data for Compounds 1−3

	1[a]		2[b]		3[c]	
position	δ_H (J in Hz)	δ_C	δ_H (J in Hz)	δ_C	δ_H (J in Hz)	δ_C
1	2.18−2.15 m Hα, 0.64 t (11.9) Hβ	46.9, CH_2	2.20−2.15 m Hα, 0.73−0.67 m Hβ	50.4, CH_2	2.19 ddd (12.2, 4.5, 1.7) Hα, 0.73 t (11.7) Hβ	48.6, CH_2
2	4.06−4.00 m, overlapped	72.4, CH[d]	4.20−4.13 m	65.1, CH	4.25 ddd (15.8, 11.2, 4.5)	64.4, CH
3	2.23 dd (2.19, 1.75), 1.07 ddd (5.41, 5.30, 4.74)	34.2, CH_2	2.40−2.35 m, 1.27−1.23 m	38.3, CH_2	2.44−2.40 m, 1.26−1.24 m (2H)	37.6, CH_2
4	2.57 bs	45.5, CH_2	2.65 bs	44.9, CH	2.70 ddd (10.4, 5.2, 1.9)	43.7, CH_2
5	1.38−1.28 m (5H)	48.3, CH	1.54−1.46 m (4H)	NA[e]	1.55−1.52 m (2H)	48.4, CH
6	1.78−1.73 m, 1.56−149 m (4H)	24.9, CH_2	1.98−1.88 m, 1.71−1.61 m (4H)	26.7, CH_2	1.70−1.66 m (3H), 1.87−1.78 m (2H)	24.5, CH_2
7	1.56−149 m (4H), 1.38−1.28 m (5H)	34.7, CH_2	1.71−1.61 m (4H), 1.54−1.46 m (4H)	36.2, CH_2	1.94−1.89 m, 1.36−1.32 m	33.3, CH_2
8		47.1, C		NA[e]		52.2, C
9	0.97 d (7.9)	52.3, CH	1.06 d (7.5)	54.5, CH	1.26 − 1.24 m (2H)	50.9, CH
10		42.8, C		41.8, C		40.9, C
11	1.56−1.49 m (4H), 1.38−1.28 m (5H)	17.5, CH_2	1.71−1.61 m (4H), NA[e]	19.2, CH_2	1.70−1.66 m (3H), 1.55−1.52 m (2H)	18.3, CH_2
12	1.56−1.49 m (4H), 1.38−1.28 m (5H)	32.1, CH_2	1.71−1.61 m (4H), NA[e]	33.6, CH_2	1.87−1.79 m (2H), 1.70−1.66 m (3H)	32.1, CH_2
13	2.61 bs	41.4, CH	2.71 bs	43.7, CH	3.04 m (1H)	38.1, CH
14	1.70 d (10.9), 1.38−1.28 m (5H)	35.7, CH_2	1.90−1.87 m, 1.42−1.38 dd (4.9, 4.8)	37.2, CH_2	2.34 d (11.9), 1.42−1.37 m	36.7, CH_2
15	3.63−3.61 m	81.1, CH	3.77 s	83.6, CH		210.2, C=O
16		159.5, C		160.3, C		149.3, C
17	5.06 bs, 4.96 bs	107.6, CH_2	5.19 bs, 5.08 bs	109.1, CH_2	5.95 bs, 5.26 bs	114.9, CH_2
19		176.2, C=O		179.1, C=O		175.3, C=O
20	0.89 d (2.63, 3H)	16.3, CH_3	1.01 s (3H)	17.3, CH_3	0.96 bs (3H)	16.3, CH_3
OCH_3					3.67 bs (3H)	51.4, CH_3
1′	4.55 d (7.8)	98.9, CH				
2′	4.64 t (8.0)	72.2, CH[d]				
3′	4.31 t (8.3)	77.0, CH				
4′	4.02 t (8.5), overlapped	73.1, CH				
5′	3.45−3.42 (m)	75.8, CH				
6′	3.67−3.64 (m), 3.59−3.54 (m)	61.2, CH_2				
1″		170.8, C=O				
2″	2.14 d (2.33), 2.12 d (1.98)	42.7, CH_2				
3″	1.96 sept (6.7)	24.8, CH				
4″, 5″	0.87 d (2.5, 6H)	22.13, 22.17, CH_3				

[a]Recorded in DMSO-d_6, 500 and 125 MHz. [b]Recorded in methanol-d_4, 400 and 100 MHz. [c]Recorded in $CDCl_3$, 400 and 100 MHz. [d]Assignments may be interchanged. [e]Carbon signals C-5 and C-8 of genin **2** were previously recorded at δ_C 49.9 and 48.6, respectively.[7] NA = not assigned.

dx.doi.org/10.1021/np300080w | J. Nat. Prod. 2012, 75, 1070−1075

Scheme 2. Proposed Mechanism for the Oxidative Cleavage of the Glycosidic Bond of 6

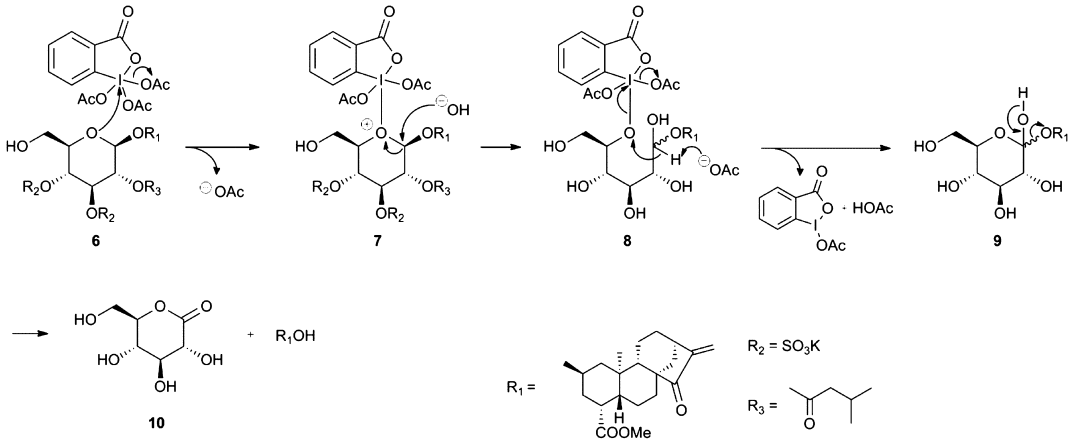

Finally, the methine carbon signal at δ_C 48.3 correlated with the remaining proton of spin system B and was assigned to C-5. Carbon assignment was followed by the identification of the A and B spin system protons. It was found that spin system A comprised H_2-6 (1H), H_2-7 (1H), H_2-11 (1H), and H_2-12 (1H), whereas spin system B included H-5 (1H), H_2-7 (1H), H_2-11 (1H), H_2-12 (1H), and H_2-14 (1H).

At this stage, the low-field region of the ^{1}H NMR spectrum of atractyloside was investigated and glucose-proton signals at δ_H 4.55 (d, J = 7.8 Hz), 4.31 (t, J = 8.3 Hz), and 3.45−3.42 (m) were assigned to H-1′, H-3′, and H-5′, respectively (Table 1). Superimposed signals at δ_H 4.06−4.00 (m, 2H) and three multiplets at δ_H 3.67−3.64 (1H), 3.63−3.61 (1H), and 3.59−3.54 (1H) were analyzed using long-range (HMBC) and through-bond (HSQC) heteronuclear correlation experiments.

Two triplets, δ_H 4.64 (J = 8.0 Hz, 1H) and 4.02 (J = 8.5 Hz, slightly overlapped) correlated with three carbon signals at δ_C 72.2, 72.4, and 73.1. The triplet at δ_H 4.64 was assigned to H-2′ due to its ^2J long-range correlations (HMBC) with C-3′ (δ_C 77.0) and C-1′ (δ_C 98.9) and a ^3J correlation with C-1″ (δ_C 170.8) of the isovaleric residue (Figure 2). Furthermore, the

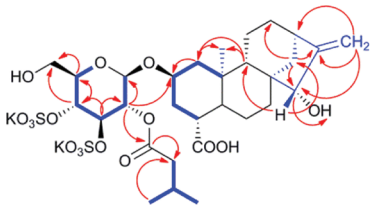

Figure 2. ^{1}H−^{1}H COSY (blue lines) correlations and key HMBC (red arrows) for **1**.

triplet at δ_H 4.02, which was overlapped with the H-2 signal, was assigned to H-4′ of the carbohydrate unit of **1**. Further sets of connectivities (HSQC) were observed between one methylene carbon signal at δ_C 61.2 and two multiplets at δ_H 3.67−3.64 and 3.59−3.54 and between the methine carbon signal at δ_C 81.1 and the multiplet at δ_H 3.63−3.61. This multiplet (δ_H 3.63−3.61) also showed HMBC correlations with C-9 (δ_C 52.3) and C-14 (δ_C 35.7) and was assigned to H-15, whereas the carbon signal at δ_C 61.2 was assigned to C-6′ due to its long-range correlations with H-4′ and H-5′ (Figure 2). Final assignment of proton resonances of the isovaleric acid residue completed the first structure elucidation of atractyloside **1** by NMR spectroscopy (Table 1).

X-ray crystallographic analysis allowed determination of the configurations of (−)-atractyloside, and the resulting ORTEP drawings are presented in Figure 3a,b. The crystallographic experiments established the configuration 2*R**, 4*R**, 5*R**, 8*R**, 9*S**, 10*R**, 13*R**, 15*S**, 1′*S**, 2′*R**, 3′*R**, 4′*R**, and 5′*R**. Moreover, observation of the stick model in Figure 3b revealed that the perhydrophenanthrene portion of **1** has little conformational flexibility. The cyclohexane rings A, B, and C all adopt a chair conformation, with the A and B rings being *trans* fused and B and C rings *cis* fused. The cyclopentane D ring is in turn fused to the C ring to form a bicyclo[3.2.1]-octane cage with the methylene and hydroxy groups sticking out from the periphery of the molecule. The α-oriented C-19 carboxylic and C-20 methyl residues of the *ent*-kaurane moiety and the β-oriented C-2−O-5−C-1′ bridge are also clearly evident in Figure 3b.

Interestingly, it was also observed that the crystal asymmetric unit of atractyloside contained three equivalent molecules coordinated to six metal ions. As a result, three sets of positional parameters and bond distances/angles were obtained, and these data could be employed, at a later stage, to aid in the determination of the most thermodynamically favorable conformation of **1**. This could further lead to in silico molecular modeling studies on the interaction of atractyloside with its biological target and to the synthesis of analogues with improved efficacy.

Compounds **1**−**3** were evaluated in vitro for their antimicrobial activity against *E. coli*, *Ent. faecalis*, and several strains of *Staph. aureus*, some of which were multidrug- and methicillin-resistant (MRSA), and minimum inhibitory concentration (MIC) values were determined. Only compound **3** exhibited moderate antibiotic activity (128 mg/L) against a susceptibility testing control strain (ATCC 29523), a fluoroquinolone-resistant derivative (SA1199B), and two epidemic-MRSA (EMRSA-15 and -16) isolates of *Staph. aureus*.

EXPERIMENTAL SECTION

General Experimental Information. Optical rotations were determined on a Bellingham and Stanley polarimeter ADP 220. Infrared spectra were acquired on a Perkin-Elmer FT-IR spectrometer (Spectrum 1000), and absorbance frequencies are reported in reciprocal centimeters (cm^{-1}). ^{1}H and ^{13}C NMR spectra were acquired using Bruker Avance 400 and 500 NMR spectrometers. Chemical shifts are reported in parts per million (ppm) with the solvent resonance as the internal standard, and coupling constants (J) are quoted in hertz (Hz). Spin multiplicities are described as s

dx.doi.org/10.1021/np300080w | J. Nat. Prod. 2012, 75, 1070−1075

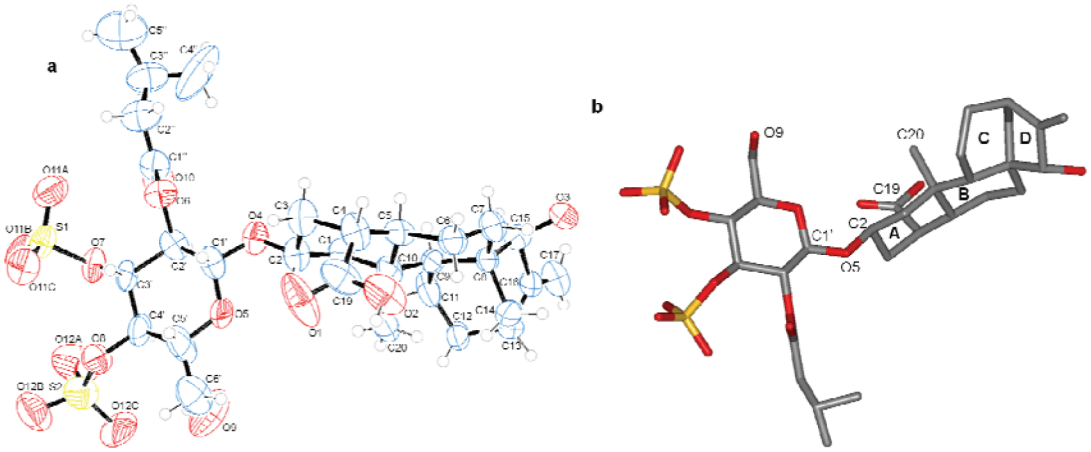

Figure 3. ORTEP[24] representations of one molecule of atractyloside (**1**): (a) with thermal ellipsoids drawn at 50% probability, hydrogen atoms drawn as spheres modeled with idealized geometry, and (b) in a stick model. Only non-hydrogen atoms are given.

(singlet), bs (broad singlet), d (doublet), dd (doublet of doublets), ddd (doublet of doublets of doublets), t (triplet), q (quadruplet), sept (septet), and m (multiplet). LC-MS analyses were carried out on a Phenomenex Monolithic C_{18} reversed-phase column (50 × 4.6 mm) with a flow rate of 3 mL min^{-1} and a linear gradient of B (5−95%) over 5 min. Eluent A: H_2O/0.1% formic acid; eluent B: CH_3CN/0.1% formic acid. TLC was performed on Merck silica gel 60 F_{254} aluminum sheets. TLC system 1: silica gel, EtOAc/acetone/H_2O:HOAc, 5:3:1:1, sprayed with a vanillin/H_2SO_4 solution prepared by dissolving 15 g of vanillin in 250 mL of EtOH with 0.01% concentrated H_2SO_4. TLC system 2: Si gel, $CHCl_3$/MeOH/HOAc, 8:2:0.5. Preparative TLC was performed on Merck silica gel 60 F_{254}, 2 mm, 20 × 20 cm plates. All chemicals were purchased from Fisher Scientific, Sigma Aldrich, and Merck Chemicals and used without further purification. Atractyloside potassium salt (**1**) was purchased from Enzo Life Science (batch no. P4432) and Sigma Aldrich and characterized prior to synthetic modification.

Chemistry. *Characterization of atractyloside potassium salt (1):* amorphous solid; TLC (system 1) R_f 0.45 (purple); $[\alpha]_D^{20}$ −52.5 (*c* 0.2, H_2O); IR ν_{max} (golden gate) cm^{-1} 3454, 2930, 1709, 1705, 1247, 1031, 909, 795; ^1H NMR and ^{13}C NMR (DMSO-d_6) see Table 1; ESIMS *m*/*z* (negative mode) 725 $[M - H]^-$, 645 $[M - SO_3 - H]^-$, 362, 322.

Synthesis of Atractyligenin (2). Atractyloside potassium salt (**1**) (0.056 mmol, 45 mg) was added to a solution of KOH (1 g, 0.018 mol) in H_2O (5 mL). The reaction mixture was allowed to stir at reflux (100 °C) for 6 h. After acidification with 10% HCl to pH = 3, the genin was extracted with EtOAc (3 × 10 mL) and dried over $MgSO_4$, and the solvent was evaporated under reduced pressure to yield 15 mg (0.047 mmol, 84%) of a white residue. The product was judged pure by analysis of TLC, LC-MS, NMR, and IR spectra. TLC (system 2): R_f 0.17; $[\alpha]_D^{20}$ −145 (*c* 0.2, EtOH); IR ν_{max} (golden gate) cm^{-1} 3420, 1701, 1658, 910; ^1H NMR and ^{13}C NMR (MeOD) see Table 1; ESIMS *m*/*z* (negative mode) 319 $[M - H]^-$.

Synthesis of Atractyloside Methyl Ester (5). To a solution of atractyloside potassium salt (**1**) (100 mg, 0.124 mmol) in a mixture of dry THF/MeOH (4:1, 5 mL) was added $TMSCH_2N_2$ (93 μL, 0.186 mmol, 2.0 M in Et_2O) dissolved in 0.5 mL of dry MeOH over a period of 5 min at −40 °C (MeCN/dry ice cooling bath). The reaction mixture was allowed to reach room temperature and then stirred for a further 3 h. The mixture was filtered on a pad of Si gel and eluted with MeOH (15 mL). The solvent was evaporated under reduced pressure to yield 48 mg of **5** as a white solid (0.058 mmol, 47.5%), which was judged pure by analysis of TLC, LC-MS, NMR, and IR spectra. $[\alpha]_D^{20}$ −40.0 (*c* 0.1, MeOH); TLC (system 1) R_f 0.54 (pink); ^1H NMR (400 MHz, MeOD) δ_H 5.17 (bs, 1H), 5.07 (bs, 1H), 4.92−4.87 (m, 1H), 4.71 (d, *J* = 8.0 Hz, 1H), 4.59−4.54 (m, 2H), 4.32 (t, *J* = 9.4 Hz, 1H), 4.26−4.21 (m, 1H), 3.94 − 3.83 (m, 2H), 3.76 (s, 1H), 3.66 (s, 3H), 3.56−3.50 (m, 1H), 2.71 (bs, 1H), 2.45 (d, *J* = 11.1 Hz, 1H), 2.34−2.29 (m, 1H), 2.28 (d, *J* = 7.2 Hz, 2H), 2.08 (sept, *J* = 6.8 Hz, 1H), 1.87−1.78 (m, 2H), 1.69−1.56 (m, 4H), 1.46−144 (m, 4H), 1.41−1.39 (m, 2H), 1.38−1.35 (m, 2H), 1.26−1.22 (m, 2H), 1.05 (d, *J* = 7.1 Hz, 1H), 0.96 (dd, *J* = 6.7, 2.1 Hz, 6H), 0.90 (s, 3H), 0.77 (t, *J* = 11.9 Hz, 1H); ^{13}C NMR (400 MHz, MeOD) δ_C 177.0, 174.1, 160.4, 109.1, 83.6, 79.9, 77.4, 76.3, 75.4, 73.5, 73.3, 64.4, 61.7, 54.5, 51.8, 50.6, 46.8, 44.8, 44.6, 43.7, 41.6, 37.3, 36.2, 35.5, 33.6, 30.7, 26.4, 24.8, 23.0, 19.2, 17.2; ESIMS *m*/*z* (negative mode) 739 $[M - H]^-$, 659 $[M - SO_3 - H]^-$, 368; HR-ESIMS (*m*/*z*) 739.2299 $[M - H]^-$ (calcd for $C_{31}H_{46}O_{16}S_2$, 739.2306).

Synthesis of 15-Didehydroatractyligenin Methyl Ester (3). To a solution of atractyloside methyl ester (**1**) (47.7 mg, 0.058 mmol) in dry CH_2Cl_2 (10 mL) was added neat Dess-Martin periodinane reagent (90.75 mg, 0.213 mmol) in one portion at 0 °C. The reaction mixture was allowed to reach room temperature and stirred under a nitrogen atmosphere for 3 h. The reaction was quenched with 1.5 M NaOH (5 mL), allowed to stir for a further 45 min at room temperature, and extracted with EtOAc (3 × 5 mL). The combined organic fractions were washed with 1.5 M NaOH (3 × 5 mL) and brine (2 × 5 mL), dried over $MgSO_4$, and evaporated under reduced pressure to yield a white solid. Purification by preparative TLC ($CHCl_3$−0.4% MeOH, R_f = 0.34) afforded **3** as a white, crystalline solid (10 mg, 0.030 mmol, 52%): $[\alpha]_D^{20}$ −171.4 (*c* 0.1, $CHCl_3$); IR ν_{max} (golden gate) cm^{-1} 3430, 3063, 2940, 1710, 1670, 1650, 1435, 1270, 1201, 1195, 1050, 938; ^1H NMR and ^{13}C NMR ($CDCl_3$) see Table 1; ESIMS *m*/*z* (positive mode) 333 $[M + H]^+$.

X-ray Diffractometry. Large, rod-shaped crystals of atractyloside (**1**) were grown by recrystallization from DMSO under oil drops over several days at 12 °C. Data were collected at 105 K on a single flash-frozen crystal processed and scaled using CrysalisPro.[25] The structure was solved by direct methods using SIR92[26] and refined using SHELXL97[27] from 10 377 independent reflections. All non-hydrogen atoms were refined by full-matrix, least-squares with anisotropic temperature factors, with hydrogen atoms positioned using normal geometry.

Crystallographic data of atractyloside (1): colorless crystal, $C_{30}S_2H_{44}K_2O_{16}$, M_r = 802.13, solvent O_5, orthorhombic, space group *C* 2 2 2_1, *a* = 22.9830(10) Å, *b* = 42.3640(22) Å, *c* = 24.0500(11) Å, $\alpha = \beta = \gamma = 90°$ *V* = 1130.57(16) $Å^3$, *Z* = 8, Cu Kα radiation, three atractyloside molecules in each ASU, crystal dimensions = 0.40 × 0.05 × 0.04 mm.

Data collection: Xcalibur microfocus NovaT X-ray diffractometer, 20 588 measured reflections, 14 053 independent reflections, 10 377 reflections with $I > 2\sigma(I)$, R_{int} = 0.045, av $I/\sigma(I)$ = 14.7.

Refinement: $R[F^2 > 2\sigma(F^2)]$ = 0.0141, $wR(F^2)$ = 0.358, *S* = 1.48, 14 053 reflections, 1392 parameters, H-atom parameters constrained, $\Delta\rho_{max}$ =1.11 e $Å^{-3}$, $\Delta\rho_{min}$ = −0.89 e $Å^{-3}$.

Crystallographic data in this paper have been deposited with the Cambridge Crystallographic Data Centre (deposition number: CCDC

873675). Copies of the data can be obtained, free of charge, on application to the Director, CCDC, 12 Union Road, Cambridge CB2 1EZ, UK (fax: +44-(0)1223-336033 or e-mail: deposit@ccdc.cam.ac.uk).

Biological Assay. *Antibacterial Assay.* Unless otherwise stated, all chemicals were obtained from Sigma-Aldrich Company Ltd., UK. Cation-adjusted Mueller-Hinton broth was obtained from Oxoid and was adjusted to contain 20 and 10 mg/L of Ca^{2+} and Mg^{2+}, respectively. The *Staphylococcus aureus* strains used in this study included ATCC 25923, SA-1199B, EMRSA-15, and EMRSA-16. ATCC 25923 is a standard laboratory strain sensitive to antibiotics. SA-1199B overexpresses the NorA MDR efflux pump. EMRSA-15 and EMRSA-16 are epidemic strains in the UK. *Enterococcus faecalis* NCTC 12697 and *Escherichia coli* NCTC 10418 are antimicrobial susceptibility testing control strains and were obtained from The National Collection of Type Cultures (London, United Kingdom). *Staph. aureus*, *E. coli*, and *Ent. faecalis* strains were cultured on nutrient agar (Oxoid) and incubated for 24 h at 37 °C prior to MIC determination. An inoculum density of 5×10^5 colony forming units of each bacterial strain was prepared in normal saline (9 g/L) by comparison with a 0.5 MacFarland turbidity standard. The inoculum (125 μL) was added to all wells, and the microtiter plate was incubated at 37 °C for the corresponding incubation time. For MIC determination, 20 μL of a 5 mg/mL methanolic solution of 3-[4,5-dimethylthiazol-2-yl]-2,5-diphenyltetrazolium bromide was added to each of the wells and incubated for 20 min. Bacterial growth was indicated by a color change from yellow to dark blue. The MIC was recorded as the lowest concentration at which no growth was observed.

■ ASSOCIATED CONTENT

Supporting Information

$^1H-^{13}C$ HSQC–DEPT135 spectra showing spin systems A and B and the glucose moiety region of atractyloside in DMSO-d_6. This material is available free of charge via the Internet at http://pubs.acs.org.

■ AUTHOR INFORMATION

Corresponding Author

*Tel: +44 207 753 5800; +44 207 753 4876. E-mail: federico.brucoli@pharmacy.ac.uk; f.brucoli@ucl.ac.uk.

Notes

The authors declare no competing financial interest.

■ ACKNOWLEDGMENTS

Prof. F. Ajello is thanked for her support throughout the project.

■ REFERENCES

(1) Daniele, C.; Dahamna, S.; Firuzi, O.; Sekfali, N.; Saso, L.; Mazzanti, G. *J. Ethnopharmacol.* **2005**, *97*, 175–181.
(2) Georgiou, M.; Biol, D.; Sianidou, L.; Hatzis, T.; Papadatos, J.; Koutselinis, A. *Clin. Toxicol.* **1988**, *26*, 487–493.
(3) Fassina, G.; Contessa, A. R.; Toth, C. E. *B. Soc. Ital. Biol. Sper.* **1962**, *133*, 346–348.
(4) Hamouda, C.; Hedhili, A.; Zhioua, M.; Amamou, M. *Vet. Hum. Toxicol.* **2004**, *46*, 144–146.
(5) Lefranc, E. *C. R.* **1868**, *67*, 954–961.
(6) Popat, A.; Shear, N. H.; Malkiewicz, I.; Stewart, M. J.; Steenkamp, V.; Thomson, S.; Neuman, M. G. *Clin. Biochem.* **2001**, *34*, 229–236.
(7) Schteingart, C. D.; Pomilio, A. B. *J. Nat. Prod.* **1984**, *47*, 1046–1047.
(8) Pegel, K. H. *Chem. Eng. News* **1981**, *59*, 4.
(9) Ames, B. N. *Science* **1983**, *221*, 1256–1264.
(10) Ajello, T.; Piozzi, A.; Quilico, F.; Sprio, V. *Gazz. Chim. Ital.* **1963**, *93*, 867–915.
(11) Piozzi, F.; Quilico, A.; Ajello, T.; Sprio, V.; Melera, A. *Tetrahedron* **1966**, *22*, 515–529.
(12) Piozzi, F. In *Atractyloside: Chemistry, Biochemistry and Toxicology*; Piccin Medical Books: Padova, Italy, 1978; pp 13–32.
(13) Vignais, P. M.; Vignais, P. V.; Defaye, G. In *Atractyloside: Chemistry, Biochemistry and Toxicology*; Piccin Medical Books: Padova, Italy, 1978; pp 39–68.
(14) Roux, P.; Le Saux, A.; Fiore, C.; Schwimmer, C.; Dianoux, A. C.; Trezeguet, V.; Vignais, P. V.; Lauquin, G. J.; Brandolin, G. *Anal. Biochem.* **1996**, *234*, 31–37.
(15) Pebay-Peyroula, E.; Dahout-Gonzalez, C.; Kahn, R.; Trézéguet, V.; Lauquin, G. J. M.; Brandolin, G. *Nature* **2003**, *426*, 39–44.
(16) Camarda, L.; Di Stefano, V.; Schillaci, D. *Pharmazie* **2002**, *57*, 374–376.
(17) D'Ancona, S.; Magon, M.; Milanesi, C.; Santi, E. *Fitoterapia* **1989**, *60*, 509–517.
(18) Kedrov, A.; Hellawell, A. M.; Klosin, A.; Broadhurst, R. B.; Kunji, E. R. S.; Müller, D. J. *Structure* **2010**, *18*, 39–46.
(19) Macleod, J. K.; Gaul, K. L.; Oelrichs, P. B. *Aust. J. Chem.* **1990**, *43*, 1533–1539.
(20) Lee, S.; Shamon, L. A.; Chai, H. B.; Chagwedera, T. E.; Besterman, J. M.; Farnsworth, N. R.; Cordell, G. A.; Pezzuto, J. M.; Kinghorn, A. D. *Chem.-Biol. Interact.* **1996**, *99*, 193–204.
(21) Hanson, J. R. *Nat. Prod. Rep.* **1984**, *1*, 533–544.
(22) Rosselli, S.; Bruno, M.; Maggio, A.; Bellone, G.; Chen, T. H.; Bastow, K. F.; Lee, K. H. *J. Nat. Prod.* **2007**, *70*, 347–352.
(23) Lee, K. H.; Hall, I. H.; Mar, E. C.; Starnes, C. O.; ElGebaly, S. A.; Waddell, T. G.; Hadgraft, R. I.; Ruffner, C. G.; Weidner, I. *Science* **1977**, *196*, 533–536.
(24) Ortep-3 for Windows. Farrugia, L. J. *J. Appl. Crystallogr.* **1997**, *30*, 565.
(25) *CrysAlis PRO*; Agilent Technologies UK Ltd: Yarnton, England, 2011.
(26) Altomare, A.; Cascarano, G.; Giacovazzo, C.; Guagliardi, A. *J. Appl. Crystallogr.* **1993**, *26*, 343–350.
(27) Sheldrick, G. M.; Schneider, T. R. *Macromol. Crystallogr. Part B* **1997**, *277*, 319–343.